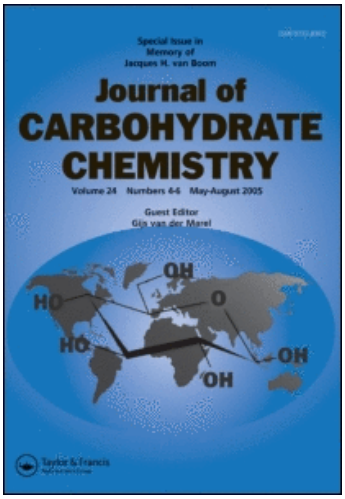

Journal of Carbohydrate Chemistry

Publication details, including instructions for authors and subscription information:
http://www.informaworld.com/smpp/title~content=t713617200

CP/MAS Carbon-13 NMR Study of Spin Relaxation Phenomena of Cellulose Containing Crystalline and Noncrystalline Components

F. Horii[a]; A. Hirai[a]; R. Kitamaru[a]
[a] Institute for Chemical Research, Kyoto University Uji, Kyoto, Japan

To cite this Article Horii, F. , Hirai, A. and Kitamaru, R.(1984) 'CP/MAS Carbon-13 NMR Study of Spin Relaxation Phenomena of Cellulose Containing Crystalline and Noncrystalline Components', Journal of Carbohydrate Chemistry, 3: 4, 641 — 662

To link to this Article: DOI: 10.1080/07328308408057922

URL: http://dx.doi.org/10.1080/07328308408057922

J. CARBOHYDRATE CHEMISTRY, 3(4), 641-662 (1984)

CP/MAS CARBON-13 NMR STUDY OF SPIN RELAXATION PHENOMENA OF CELLULOSE CONTAINING CRYSTALLINE AND NONCRYSTALLINE COMPONENTS

F. Horii*, A. Hirai, and R. Kitamaru

Institute for Chemical Research, Kyoto University
Uji, Kyoto 611, Japan

Received March 16, 1984

ABSTRACT

Cross-polarization, ^{13}C rotating frame spin-lattice relaxation and ^{13}C laboratory frame spin-lattice relaxation processes have been studied for different cellulose samples by CP/MAS ^{13}C NMR spectroscopy. It was found that the CP process can be described by a simple thermodynamic model and relative intensities of the respective resonance lines are consistent with the atomic ratios for the spectra obtained at a contact time of about 1 ms. The observed rotating frame spin-lattice relaxation times $T_{1\rho}^{C*}$ were dominantly dependent on the time constant T_{CH}^{D} by which ^{13}C nuclei were coupled to the ^{1}H dipolar spin system. It was, therefore, impossible to obtain information about molecular

 0732-8303/84/0304-0641$3.50/0

motion of cellulose from $T_{1\rho}^{C*}$. On the other hand, spin-lattice relaxation times T_1^C in the laboratory frame were found to be useful for the characterization of the structure of the crystalline and noncrystalline components of cellulose. The resonance lines assignable to the respective components were selectively recorded by use of the difference in T_1^C.

INTRODUCTION

It is well known that the combination of cross-polarization (CP),[1,2] dipolar decoupling (DD),[3] and magic-angle sample spinning (MAS)[4,5] produces high-resolution ^{13}C NMR spectra in organic solids.[6,7] The spectra are usually well resolved, and chemical shifts and various kinds of relaxation times can be determined for the respective carbons. These parameters have proved extremely useful in characterizing the local structure and molecular motion of organic compounds. However, in semi-crystalline polymers, such as cellulose, such characterization is not straight forward because the contributions from the crystalline and noncrystalline components may be overlapped or in some cases averaged out. Furthermore, the cross-polarization technique used to enhance the signal intensities may make the quantitative analyses difficult because the atomic ratios are not always reflected in the relative intensities of the spectra.

In this paper we first analyze the CP process of different cellulose samples in detail and discuss the conditions necessary to obtain signal intensities proportional to the number of carbons. Next we study the ^{13}C rotating-frame spin-relaxation process and clarify the contributions of spin-lattice effects associated with molecular motion and spin-spin effects between the ^{13}C rotating-frame Zeeman system and the proton dipolar system. Finally we show the spin-lattice relaxation times T_1^C of different cellulose samples and discuss the structure of crystalline and noncrystalline components. The measurements of the respective spectra of these two components are carried out using their different relaxation times.

RESULTS AND DISCUSSION

A. Cross-Polarization Dynamics and Quantitative Measurements of Resonance Intensities.

In the matched Hartmann-Hahn CP experiment the ^{13}C spin-locked system (rotating frame ^{13}C Zeeman system) is coupled to the lattice and to the ^{1}H spin-locked system (rotating frame ^{1}H Zeeman system) as shown schematically in Figure 1. In this case the inverse spin temperatures, β_C and β_H, (defined as $\hbar/kT$) for the respective systems vary as[8,9]

$$\frac{d\beta_C}{dt} = -\frac{\beta_C-\beta_H}{T_{CH}} - \frac{\beta_C}{T_{1\rho}^{C}} \tag{1}$$

$$\frac{d\beta_H}{dt} = -\varepsilon'\frac{\beta_H-\beta_C}{T_{CH}} - \frac{\beta_H}{T_{1\rho}^{H}} \tag{2}$$

with

$$\varepsilon' = \frac{C_C B_{1C}^{2}}{C_H B_{1H}^{2}} \tag{3}$$

where T_{CH} is the ^{13}C-^{1}H cross-polarization time constant; $T_{1\rho}^{C}$ is the carbon rotating-frame spin-lattice relaxation time constant in the presence of ^{1}H dipolar decoupling; $T_{1\rho}^{H}$ is the proton rotating-frame spin-lattice relaxation time constant; C_H and C_C are Curie constants given by

$$C_H = \tfrac{1}{3}\gamma_H^2\hbar^2 I(I+1)N_H, \quad C_C = \tfrac{1}{3}\gamma_C^2\hbar^2 S(S+1)N_C; \tag{4}$$

N_H and N_C are the numbers of proton and ^{13}C spins; and B_{1H} and B_{1C} are the amplitudes of ^{1}H and ^{13}C rf fields, respectively. Since ε' is assumed to be negligibly small in the naturally abundant ^{13}C-^{1}H spin system, the coupled differential equations can be easily solved.

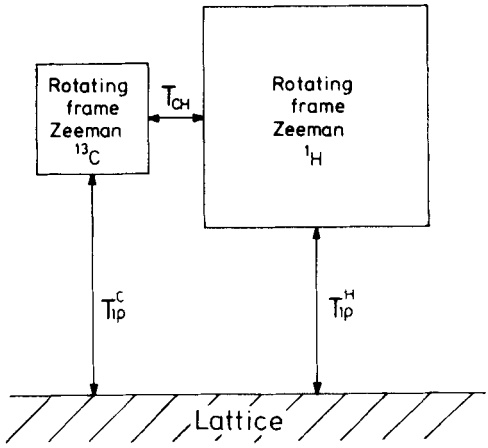

Figure 1 A thermodynamic model for the cross-polarization experiment. $T_{1\rho}^{C}$ and $T_{1\rho}^{H}$ are the spin-lattice relaxation times in the rotating frames for ^{13}C and ^{1}H nuclei, respectively, and T_{CH} is the cross-relaxation time.

On the other hand, ^{13}C magnetization S is described as

$$S = \beta_C C_C B_{1C} \tag{5}$$

Therefore, the ^{13}C magnetization in the spin-locked system is given as a function of contact time t with the use of the solution of Eq. 1 and 2 by[10]

$$S = (S_e/T_{CH})(1/T_{1\rho}^{C\dagger}-1/T_{1\rho}^{H})^{-1}[\exp(-t/T_{1\rho}^{H})-\exp(-t/T_{1\rho}^{C\dagger})] \tag{6}$$

with

$$(T_{1\rho}^{C\dagger})^{-1} = (T_{1\rho}^{C})^{-1}+(T_{CH})^{-1} \tag{7}$$

In this equation, S_e is the equilibrium carbon magnetization after long contact with ^{1}H reservoir with no dissipative relaxation process and therefore this value of S_e is proportional to the number of given carbons in a compound. This equation agrees with the equation derived by Stejskal et al.[11]

According to Eq. 6, the ^{13}C magnetization appears with the rate of $1/T_{1\rho}^{C\dagger}$ and disappears with the rate of $1/T_{1\rho}^{H}$. It is, therefore, indispensable for the observation of CP ^{13}C NMR spectra that $T_{1\rho}^{C\dagger}$ is shorter than $T_{1\rho}^{H}$. In addition, $T_{1\rho}^{C}$ is normally longer than $T_{1\rho}^{H}$ because the ^{13}C-^{1}H dipolar interaction determining the former process is less than the ^{1}H-^{1}H dipolar interaction determining the latter process. Under such conditions Eq. 6 reduces to

$$S = S_e[\exp(-t/T_{1\rho}^{H})-\exp(-t/T_{CH})] \quad (8)$$

As a result, S_e can be determined together with $T_{1\rho}^{H}$ and T_{CH} and the quantitative information of the composition of a compound can be obtained from the S_e value. Next we will show that Eq. 8 holds for cellulose samples and discuss the quantitative measurements of their CP/MAS spectra.

Figure 2 shows 25 MHz CP/MAS ^{13}C NMR spectra of ramie obtained by using different CP contact times. The assignments[12,13] for the C1, C4, and C6 carbons are also shown together with the structure of the basic repeating unit of cellulose. The sharp downfield and broad upfield components of the C4 and C6 carbons were assigned to the crystalline and noncrystalline components, respectively, on the basis of the fact that the integrated fraction of the upfield component was well correlated with the degree of crystallinity determined by x-ray analysis.[14,15,16] It has been confirmed as shown later that C1, and C2, C3, and C5 resonance lines also contain both components.

In Figure 3 the logarithmic peak intensities of the C1, C4, and C6 lines of ramie are plotted against the CP contact time. As is assumed by Eq. 8, the ^{13}C magnetization of each carbon is rapidly generated, passes through a maximum, and gradually decreases. Similar results have been reported for poly(ether sulfone),[7] polycarbonate,[7] piperidine-cured epoxy,[10] polyethylene,[19,20] polystyrene,[21] and styrene-butadiene block copolymers.[22] The $T_{1\rho}^{H}$ values were determined from the slopes in the region for the contact time longer than about 1 ms. The T_{CH}

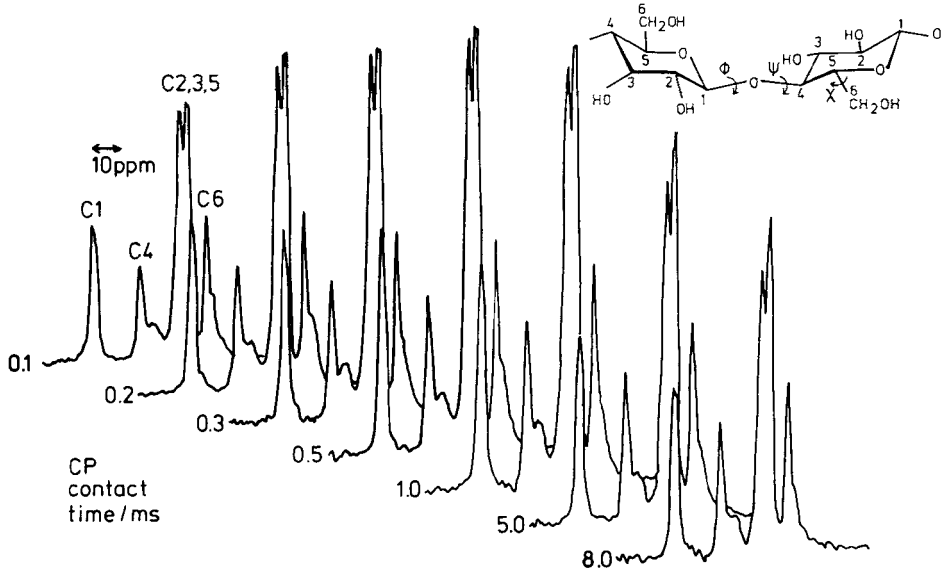

Figure 2 25 MHz CP/MAS ^{13}C NMR spectra of ramie obtained at different CP contact times.

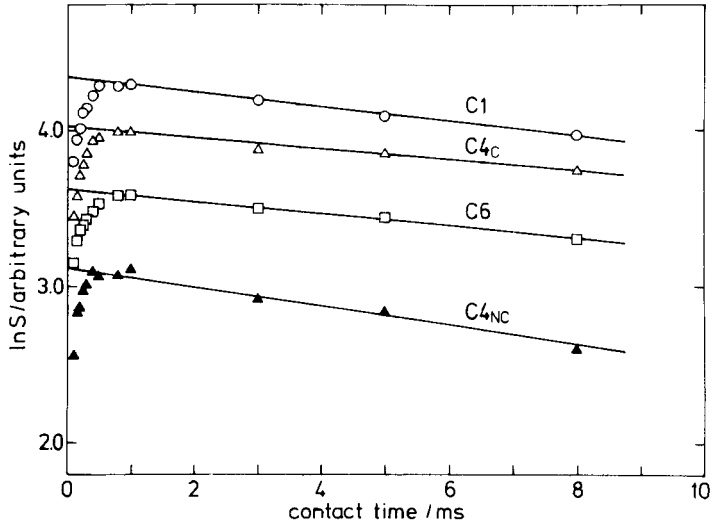

Figure 3 Semilogarithmic plots of peak intensities as a function of CP contact time for ramie.

values were determined in the following manner. For $t>5T_{CH}$ Eq. 8 approximately reduces to

$$S_L = S_e \exp(-t/T_{1\rho}^H) \quad (9)$$

which corresponds to the part described as a straight line in Figure 3. This linear part of the curve is extrapolated into the region of $t<5\ T_{CH}$ and observed values S' are substracted from the extrapolated values. If $\ln(S_L-S')$ is plotted against the contact time, T_{CH} can be obtained from the slope. Such semilogarithmic plots are shown in Figure 4. Since straight lines are obtained for the respective carbons, it is concluded that the simple expression described by Eq. 8 can be applied to the cross-polarization experiment of ramie cellulose.

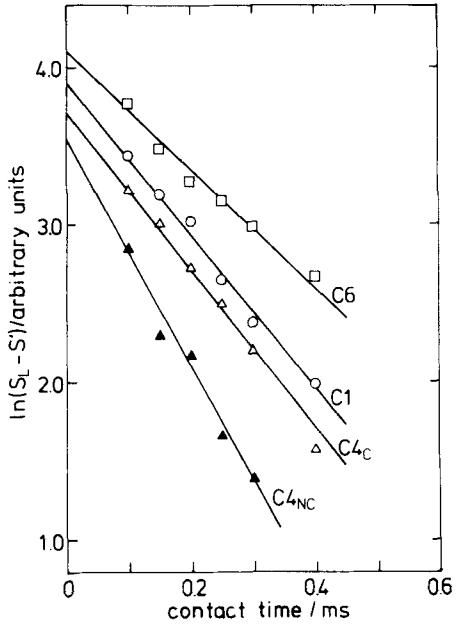

Figure 4 Semilogarithmic plots of S_L-S' as a function of CP contact time for ramie.

TABLE 1.

Spin Relaxation Parameters in the Matched Hartmann-Hahn Cross-Polarization Experiments for Ramie.

carbon	T_{CH} [c] /ms	$T_{1\rho}^{H}$ [c] /ms
C1	0.21	21
$C4_C$ [a]	0.20	29
$C4_{NC}$ [b]	0.14	15
C6	0.26	26

a) crystalline component, b) noncrystalline component, c) Determined from the slopes of the lines shown in Figures 4 and 3, respectively.

In Table 1 the T_{CH} ane $T_{1\rho}^{H}$ values thus obtained are summarized. The T_{CH} values are about 1/100 of the $T_{1\rho}^{H}$ values for the respective carbons, indicating that the approximation ($T_{CH} << T_{1\rho}^{H} < T_{1\rho}^{C}$) which was used to derive Eq. 8 is valid for ramie. On the other hand, the differences in T_{CH} and $T_{1\rho}^{H}$ are not so significant among the carbons except for the noncrystalline C4 carbon ($C4_{NC}$). The $T_{1\rho}^{H}$ of the $C4_{NC}$ is about half of that of the crystalline C4 carbon ($C4_C$). This suggests that the diffusion of proton spins between the two phases is not so high as to average out their $T_{1\rho}^{H}$ values. Nevertheless, since such differences are very small, it is difficult to discriminate the noncrystalline components in T_{CH} and $T_{1\rho}^{H}$ values for C1 and C6 carbons.

Since the T_{CH} and $T_{1\rho}^{H}$ values could be determined as described above, we can estimate S_e for any spectrum of ramie obtained at any contact time using Eq. 8. However, it is very tedious to perform such an analysis for each sample. If we consider the small differences in those time constants, we can get direct information about quantitative intensities of resonance lines in good approximation. For example, the value $\exp(-t/T_{1\rho}^{H}) - \exp(-t/T_{CH})$ in Eq. 8 ranges from 0.93 to 0.96 for each carbon of

ramie at the contact time of 1 ms which yields almost the maximum ^{13}C magnetization (see Figure 2). Therefore, the relative intensity of each carbon must be reflected within the error of 3% on the real spectrum obtained at the contact time of 1 ms.

Table 2 shows the relative integrated intensities of the resonance lines of the CP/MAS spectra obtained at the contact time of 1 ms for different cellulose samples. Since the upfield part of the C4 resonance line overlaps the resonance lines of the C2, C3, and C5 carbons,[14,15] the total intensities of these carbons were calculated without separation. It has been found that the intensities of the carbons except for C6 are in good accord with the theoretical values. The relatively low intensities of the C6 carbons may be due to the underestimation of the noncrystalline component.

B. ^{13}C Spin-Lattice Relaxation in the Rotating Frame

The ^{13}C spin-lattice relaxation process in the rotating frame is easy to observe because of the rapid relaxation rate in comparison with the spin-lattice relaxation process in the

TABLE 2.

Relative Integrated Intensities of the Resonance Lines in CP/MAS ^{13}C NMR Spectra of Different Cellulose Samples.

samples	relative integrated intensities		
	C1	C2 + C3 + C4 + C5	C6
Theoretical	1	4	1
Experimental			
ramie	1.0	4.0	1.0
cotton	1.0	4.1	0.89
bacterial	1.0	4.1	0.87
rayon fibers	1.0	3.9	0.74

laboratory frame. In this case, the spin-locked carbon system is linked to the ^1H dipolar reservior[23] in place of the spin-locked ^1H system in the CP experiment shown in Figure 1. Since the time constant T_{1D}^H by which the ^1H dipolar reservior is coupled to the lattice may become very short under MAS, the observed spin-lattice relaxation time $T_{1\rho}^{C*}$ is given by

$$(T_{1\rho}^{C*})^{-1} = (T_{1\rho}^{C'})^{-1} + (T_{CH}^{D})^{-1} \tag{10}$$

where $T_{1\rho}^{C'}$ and T_{CH}^{D} are the time constants by which the carbon system is coupled to the lattice and to the proton dipolar reservior, respectively. We studied which contribution dominates $T_{1\rho}^{C*}$ for the crystalline and noncrystalline components of ramie by analyzing the lock field dependences of the $T_{1\rho}^{C*}$.

Figure 5 shows the decay of ^{13}C magnetization locked with the field intensity ν_{1C} of 69 kHz in the rotating frame for ramie. Except for the small deviations in the region of short τ values for C1, $C4_C$, and C6 carbons, the semilog plots of the peak heights vs. τ yield straight lines. The $T_{1\rho}^{C*}$ values are determined from the slopes to be 80, 82, 39, and 35 ms for C1, $C4_C$, C6, and $C4_{NC}$ carbons, respectively.

Somewhat rapid decreases in magnetization appearing at short τ values may be due to the contributions of the noncrystalline components. However, since the reliable $T_{1\rho}^{C*}$ value of the component is difficult to obtain for the C1 and C6 carbons, only the $T_{1\rho}^{C*}$ of the $C4_{NC}$ carbon is treated here as a noncrystalline component of ramie.

In Figure 6 the logarithmic $T_{1\rho}^{C*}$ values obtained at different field intensities ν_{1C} are plotted against ν_{1C}. Straight lines are obtained for the respective carbons including the $C4_{NC}$ carbon. It is, therefore, concluded that the $T_{1\rho}^{C*}$ is dominated not by the $T_{1\rho}^{C'}$ but by the T_{CH}^{D} (see Eq. 10). The reason is that the former process is dependent on ν_{1C}^2, while the latter process has an exponential field dependence.[23] Such a high contribution of the T_{CH}^{D} process has also been observed for the crystalline components

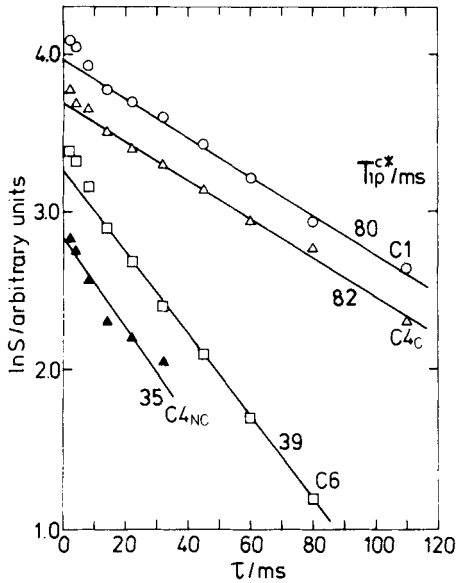

Figure 5 Semilogarithmic plots of ^{13}C spin-locked magnetization as a function of spin-lock time τ for ramie. The spin-lock field intensity ν_{1C} was 69 kHz.

of polyethylene[23] and polyoxymethylene.[11] On the other hand, in glassy polymers such as polystyrene,[11] poly(methyl methacrylate),[11] poly(2,6-dimethyl phenylene oxide),[11] and piperidine-cured epoxy[24] the $T_{1\rho}^{C'}$ process dominates the observed $T_{1\rho}^{C*}$ process. It should be, therefore, noted that the $T_{1\rho}^{C*}$ of the noncrystalline component of ramie is determined by the T_{CH}^{D} process.

Finally we summarize the order of the respective time constants relating to the ^{13}C spin-locked systems for ramie;

$$T_{1\rho}^{C} > T_{1\rho}^{C'} >> T_{CH}^{D} \sim T_{1\rho}^{C*} \text{ (35-80 ms)}$$

$$> T_{1\rho}^{H} \text{ (15-29 ms)} >> T_{CH} \text{ (0.14-0.26 ms)}$$

where $T_{1\rho}^{C}$ is assumed to be sensitive to the fluctuation of the C-H vector not at $2\pi\nu_{1C}$ but at $4\pi\nu_{1C}$.[10]

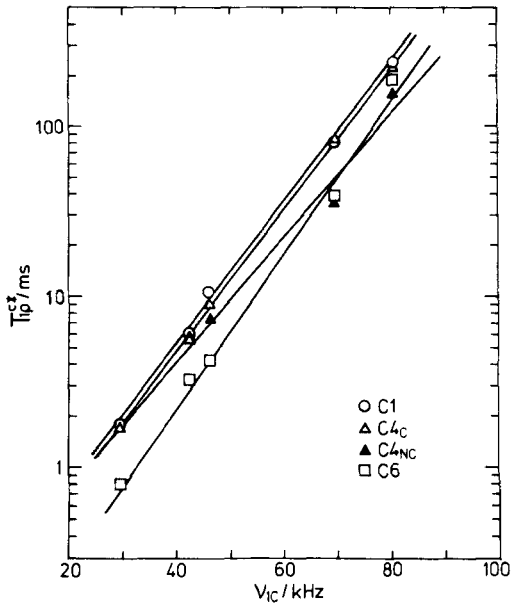

Figure 6 The dependence of ^{13}C rotating frame relaxation time, $T_{1\rho}^{C*}$, on the ^{13}C rf field intensity ν_{1C} for ramie.

c. ^{13}C Spin-Lattice Relaxation in the Laboratory Frame and Selective Observation of the Crystalline and Noncrystalline Resonance Lines.

Figure 7 shows the semilogarithmic decay curves of the respective peak intensities in ^{13}C spin-lattice relaxation in the laboratory frame which were obtained for ramie by using the pulse sequence shown in Figure 10(b). It is clear that each decay curve except for the C4 carbon is composed of two components with different T_1^C values. These two components correspond to the two components of the C4 carbon which have different chemical shifts and therefore are observable as different decay curves. Since it has been confirmed as mentioned above that the two components of the C4 carbon are the crystalline and noncrystalline components,[14,15] it is concluded that the long T_1^C and short T_1^C

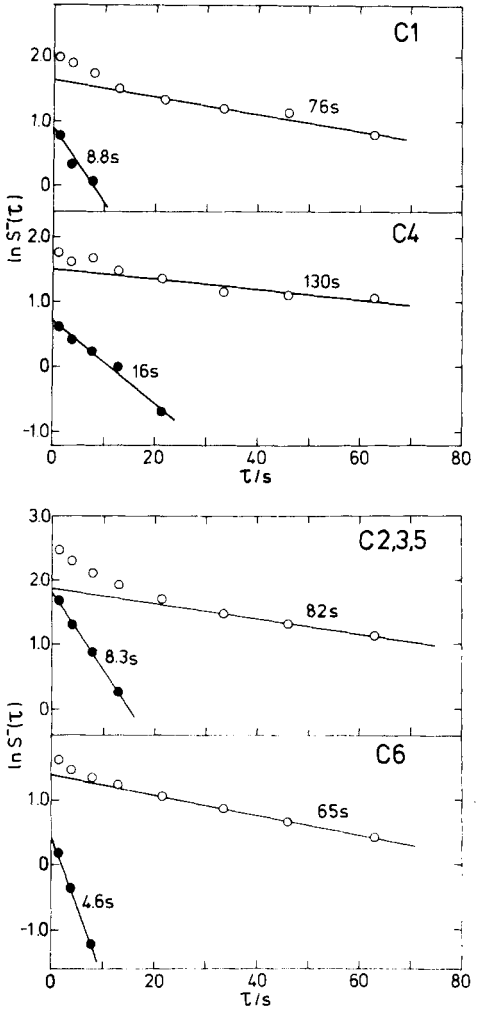

Figure 7 Semilogarithmic plots of $S^{-}(\tau)$ vs. τ, which were obtained by using the pulse sequences shown in Figure 10(b) in order to measure the spin-lattice relaxation time T_1^C in the laboratory frame.

TABLE 3.

^{13}C Spin-Lattice Relaxation Times of the Carbons of Different Cellulose Samples.

Sample	T_1/s							
	C1		C4		C6		C2, 3, 5	
ramie	76	8.8	130	16	65	4.6	82	8.3
cotton	78	~7	87	11	89	~7	67	~8
bacterial	87	—	107	—	86	—	104	5.7
rayon fibers	58	6.8	82	9.9	53	4.2	37	4.7

components of the respective carbons are the crystalline and noncrystalline components, respectively.

The T_1^C values of different cellulose samples are summarized in Table 3. For all the samples studied here each carbon contains two components with different T_1^C values, although it is difficult to discern the short T_1^C component in the decay curves of bacterial cellulose except for C2, C3, and C5 carbons because of the high crystallinity. The T_1^C values of the crystalline component, which correspond to the longer values, are relatively high. However, these values are much lower than the T_1^C of the rigid crystalline component of linear polyethylene which ranges from 200s to 4600s.[19,25,26] This suggests that cellulose molecules undergo some local motion even in the crystalline phase. The T_1 values of the C4 carbon of the crystalline component seem to be longer than those of the C1 carbon. The molecular mobility of the C4-H4 vector is thought to be almost identical with that of the C1-H1 vector because the glucopyranose ring is highly restricted in inner motions. Therefore, the reason for the difference in T_1 for these carbons is not clear at present. On the other hand, the T_1 values per proton (NT_1) of the C6 carbon of the crystalline component are appreciably long in comparison with those of the ring carbons. This suggests that the CH_2OH groups do not rotate

about the exo-cyclic C5-C6 bonds in the crystalline phases. The similar results seem to be also obtained for the noncrystalline component but the features are not significant.

For the regenerated rayon fibers, the crystalline T_1^C of each carbon is clearly shorter than the corresponding value of the native cellulose samples. This may reflect the difference in crystal form; cellulose II for the regenerated cellulose and cellulose I for native cellulose.[27-30] In the previous paper[15] we have reported that these two crystal forms have different chemical shifts for the respective carbons, suggesting that they differ from each other in molecular chain conformation or in molecular chain packing. Therefore, the difference in T_1^C between cellulose I and II also may be due to the difference in molecular mobility associated with these factors. On the other hand, if ^{13}C spin diffusion,[31-33] significantly occurs between the crystalline and noncrystalline phases, the smaller size of the crystallite of the regenerated cellulose also may be related to the shorter T_1^C.

In the previous paper,[15] we have also reported by analyzing ^{13}C chemical shifts that the crystal structure of cotton and ramie differs from that of bacterial and valonia cellulose, although the same crystal form of cellulose I is assumed for these samples in the x-ray crystal analyses.[27-28] However,it is difficult to recognize the difference in T_1^C of the crystalline component among the native cellulose. Such a small difference in crystal form may not be significantly reflected on the T_1^C.

The T_1^C values of the noncrystalline component are much shorter than those of the crystalline component, ranging from 0.05 to 0.12 of the latter T_1^C. This suggests that the noncrystalline component undergoes relatively enhanced molecular motion in the order of 10^{-8}s even below the glass transition temperature. Furthermore, the slightly lower T_1^C values of the regenerated cellulose sample will be associated with our recent findings;[15] the molecular chain conformation of the noncrystalline component is rather relaxed for the regenerated cellulose, whereas it is much limited for the native cellulose samples.

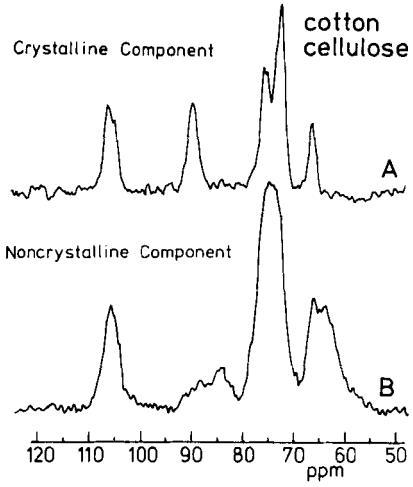

Figure 8 Partially relaxed 25 MHz ^{13}C NMR spectra of the crystalline and noncrystalline components of cotton which were separately measured by the pulse sequence for CP T1 measurement shown in Figure 10(b) and by a single π/2 pulse sequence, respectively.

Using the large difference in T_1^C between the crystalline and noncrystalline components, we tried to record selectively the spectra of the respective components. Figures 8(A) and 9(A) show the spectra of the crystalline components of cotton and bacterial celluloses which were obtained by the pulse sequence shown in Figure 10(b). The delay times τ between the two ^{13}C π/2 pulses were 42s and 46s for cotton and bacterial celluloses, respectively. The broad upfield components of C4 and C6 carbons disappear in both spectra and the fine structure of the crystalline component becomes clear in both samples. Similar results of ramie and regenerated celluloses were reported in the previous paper[15] and the crystal structure of cellulose was discussed there.

Figures 8(B) and 9(B) show the spectra of the noncrystalline components of cotton and bacterial celluloses. These spectra were

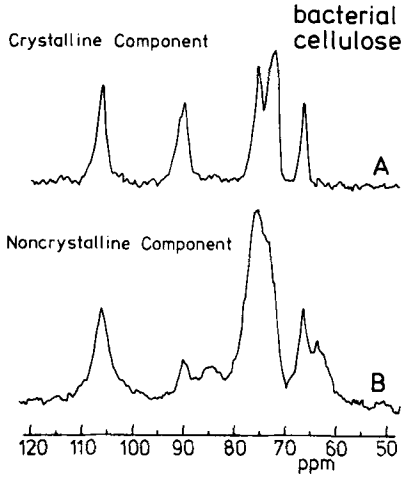

Figure 9 Partially relaxed 25 MHz ^{13}C NMR spectra of the crystalline and noncrystalline components of bacterial cellulose. The pulse sequences used were the same as for cotton shown in Figure 8.

obtained by a conventional $\pi/2$ single pulse sequence with a short waiting time of 5s employing the DD/MAS technique. As the difference in T_1^C between the crystalline and noncrystalline components is not very large, a small amount of the downfield component appears for the C4 and C6 carbons. Although the small amount of the crystalline component is also involved in each line, the features of the noncrystalline component are clear. On the basis of these results, the structure of the noncrystalline component of cellulose was discussed in the previous report.[15]

EXPERIMENTAL

A. Samples. All cellulose samples were the same as those reported in the previous papers.[14,15] These samples were dried at 50°C under vacuum for 2-3 days before and after packing in a rotor for CP/MAS measurements.

B. CP/MAS ^{13}C NMR Spectroscopy. CP/MAS ^{13}C NMR experiments were performed at room temperature by using a JEOL JNM-FX100 spectrometer operating at 25 MHz for ^{13}C. In most cases the matched field strengths ν_{1C} and ν_{1H} of 71 kHz were applied to ^{13}C and ^{1}H for 1.0 ms and the same ν_{1H} remained on during the signal acquisition period. Magic-angle sample spinning was carried out at a rate of about 3.2 kHz by use of a bullet type rotor of poly(chlorotrifluoroethylene), whose volume was about 0.5 cm^3. The spin temperature alternation method[34] was employed throughout this work involving the measurements of relaxation times in order to suppress some artifacts appearing in the CP/MAS spectra.

The observed time constant $T_{1\rho}^{C*}$ for the decay of rotating frame ^{13}C magnetization was measured by using the normal pulse sequence shown in Figure 10(a). The ^{13}C spin-lattice relaxation times T_1^C in the laboratory frame were measured with a slightly modified version (Figure 10(b)) of the T1CP method developed by Torchia.[35] In sequence A the ^{13}C magnetization was first generated by a CP procedure. Then the proton rf field ν_{1H} was turned off and at the same time the carbon magnetization was rotated to the +Z axis by an appropriate $\pi/2$ pulse. After the ^{13}C magnetization was held on for a variable time τ, the remaining magnetization was sampled under high power proton decoupling by using another appropriate $\pi/2$ pulse. During the entire delay time τ, ^{1}H $\pi/2$ pulses were applied at intervals of 20 ms in order to suppress transient nuclear Overhauser effects. Thus the ^{13}C magnetization is given by

$$S_A(\tau) = S_{CP} \exp(-\tau/T_1) - S(\infty)[1 - \exp(-\tau/T_1)] \quad (11)$$

where S_{CP} is the ^{13}C magnetization generated by the CP procedure and $S(\infty)$ is the ^{13}C equilibrium magnetization obtained for the infinite τ. In sequence B, as the ^{13}C magnetization generated by the CP procedure is rotated to the -Z axis, the observed ^{13}C magnetization is given by

$$S_B(\tau) = -S_{CP} \exp(-\tau/T_1) - S(\infty)[1 - \exp(-\tau/T_1)] \quad (12)$$

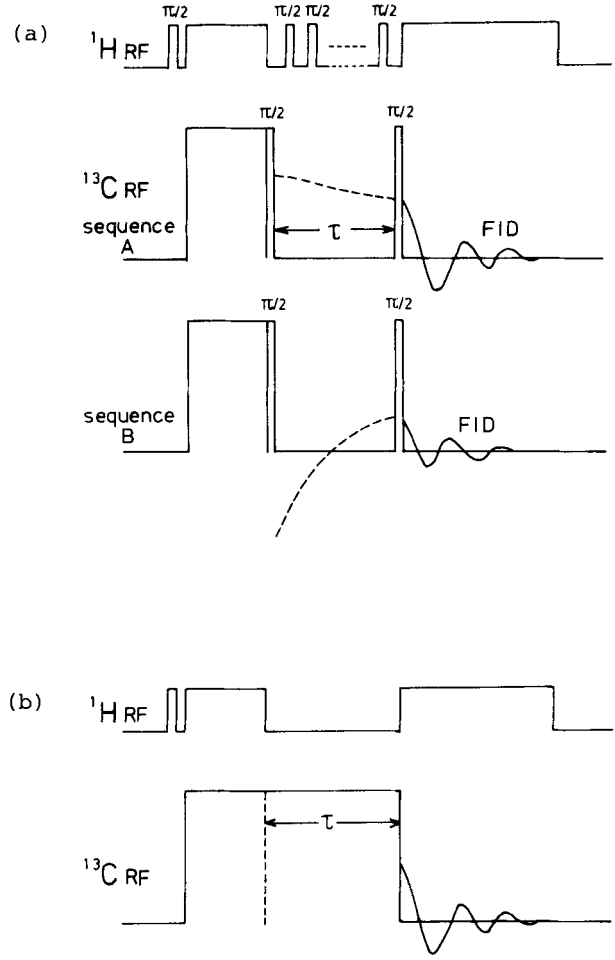

Figure 10 Pulse sequences employed for the determination of relaxation times. (a): Measurement of $T_{1\rho}^{C*}$, *(b): Measurement of* T_1^C. *The spin-temperature alternation technique was used for the respective measurements.*

If we substract Eq. 12 from Eq. 11, we obtain

$$S^{-}(\tau) = S_A(\tau) - S_B(\tau) = 2S_{CP} \exp(-\tau/T_1) \quad (13)$$

Therefore, the T_1 value can be obtained from the slope of the plot of ln $S^{-}(\tau)$ against τ without measuring the $S(\infty)$ value.

ACKNOWLEDGMENTS

This work was partly supported by the donation from Kakuyokai.

REFERENCES AND FOOTNOTES

1. S. R. Hartmann and E. L. Hahn, Phys. Rev., 128, 2042 (1962).

2. A. Pines, M. G. Gibby, and J. S. Waugh, J. Chem. Phys., 59, 569 (1973).

3. F. Bloch, Phys. Rev., 111, 841 (1958).

4. E. R. Andrew, A. Bradbury, and R. G. Eades, Nature, 182, 1659 (1958).

5. I. J. Lowe, Phys. Rev. Lett., 2, 285 (1959).

6. J. Schaefer and E. O. Stejskal, J. Am. Chem. Soc., 98, 1031 (1976).

7. J. Schaefer, E. O. Stejskal, and R. Buchdahl, Macromolecules, 10, 384 (1977).

8. D. A. McArthur, E. L. Hahn, and R. E. Walstedt, Phys. Rev., 188, 609 (1969).

9. M. Mehring, "Principles of High Resolution NMR in Solids", 2nd, Revised and Enlarged Ed.; Springer-Verlag, Berlin Heidelberg New York, 1983, p.151.

10. A. N. Garroway, W. B. Moniz, and H. A. Resing, "Carbon-13 NMR in Polymer Science", ACS Symposium Series 103; R. F. Gould, Ed.; Am. Chem. Soc., Washington D.C., 1979, p.67.

11. E. O. Stejskal, J. Schaefer, and T. R. Steger, Faraday Symp. Chem. Soc., 13, 56 (1979).

12. R. H. Atalla, J. C. Gast, D. W. Sindorf, V. J. Bartuska, and G. E. Maciel, J. Am. Chem. Soc., 102, 3249 (1980).

13. W. L. Earl and D. L. VanderHart, J. Am. Chem. Soc., 102, 3251 (1980).

14. F. Horii, A. Hirai, and R. Kitamaru, Polym. Bull., 8, 163 (1982).

15. F. Horii, A. Hirai, and R. Kitamaru, "Characterization of Fibers by Instrumental Methods", ACS Symposium Series; C. Arthur, Jr., Ed.; Am. Chem. Soc., Washington, D.C., 1984, in press.

16. There is still a controversy for the assignment of the broad upfield components of the C4 and C6 carbons. Earl and VanderHart reported in their earlier paper[36] that this component was not attributed to the noncrystalline component but to anhydroglucoses on the surface of elementary fibrils. As pointed out in our previous paper,[15] however, the basis that they denied the contribution of the noncrystalline component cannot be accepted. VanderHart and Atalla[17,18] reported very recently that the upfield component included the noncrystalline component but the surface component still contributed to it. In order to deduce this conclusion they assumed that the CP/MAS ^{13}C spectrum of the whole noncrystalline component of the native cellulose was the same as that of amorphous cellulose such as ball-milled Whatman CF1 cellulose. However, it is more plausible that the content of the noncrystalline component such as conformation and orientation differs from sample to sample. According to our analysis[14,15] in which a Lorentzian line shape was assumed for the respective components of the resonance lines, the upfield and downfield components were assigned to the noncrystalline and crystalline components as mentioned in the text. The contribution of the surface component is thought to be small, if any.

17. D. L. VanderHart and R. H. Atalla, TAPPI Proceedings, 1983, p.207.

18. R. H. Atalla and D. L. VanderHart, Science, 223, 283 (1984).

19. B. Schroeter and A. Posern, Makromol. Chem., 3, 623 (1982).

20. F. Horii, K. Murayama, and R. Kitamaru, unpublished results.

21. T. Akita, F. Horii, and R. Kitamaru, Polym. Prepr., Japan, 32, 2549 (1983).

22. T. Akita, F. Horii, and R. Kitamaru, Polym. Prepr., Japan, 32, 827 (1983).

23. D. L. VanderHart and A. N. Garroway, J. Chem. Phys., 77, 2773 (1979).

24. A. N. Garroway, W. B. Moniz, and H. A. Resing, Faraday Symp. Chem. Soc., 13, 63 (1979).

25. R. Kitamaru, F. Horii, and K. Murayama, Polym. Bull., 7, 583 (1982).

26. R. Kitamaru, F. Horii, and K. Murayama, Polym. Prepr., Japan, 33, 713 (1984).

27. K. H. Gardner and J. Blackwell, Biopolymers, 13, 1975 (1974).

28. C. Woodcock and A. Sarko, Macromolecules, 13, 1183 (1980).

29. A. J. Stipanovic and A. Sarko, Macromolecules, 9, 851 (1976).

30. F. J. Kolpak and J. Blackwell, Macromolecules, 9, 273 (1976).

31. D. E. Axelson, L. Madelkern, R. Popli, and P. Mathieu, J. Polym. Sci. Polym. Phys. Ed., 21, 2319 (1983).

32. N. M. Szeverenyi, M. J. Sullivan, and G. E. Maciel, J. Magn. Reson., 47, 462 (1983).

33. C. E. Bronniman, N. M. Szeverenyi, and G. E. Maciel, J. Chem. Phys., 79, 3694 (1983).

34. E. O. Stejskal and J. Schaefer, J. Magn. Reson., 18, 560 (1975).

35. D. A. Torchia, J. Magn. Reson., 30, 613 (1978).

36. W. L. Earl and D. L. VanderHart, Macromolecules, 14, 570 (1981).